

# Neutron-Induced Activation Cross Sections Measurements on Molybdenum Isotopes in the 7–15 MeV Energy Range

**V. Semkova<sup>1</sup>, R. Nolte<sup>2</sup>, S. Peneva<sup>1</sup>, T. Troev<sup>1</sup>**

<sup>1</sup>Institute for Nuclear Research and Nuclear Energy,  
Bulgarian Academy of Sciences, 1784 Sofia, Bulgaria

<sup>2</sup>Physikalisch-Technische Bundesanstalt (PTB), 38116 Braunschweig, Germany

**Abstract.** Accurate neutron-induced activation cross-section data are important in many fields of science and applications. Activation cross-sections measurements of the  $^{92}\text{Mo}(n, \alpha)^{89}\text{Zr}$ ,  $^{95}\text{Mo}(n, p)^{95}\text{Nb}^m$ ,  $^{100}\text{Mo}(n, \alpha)^{97}\text{Zr}$ ,  $^{100}\text{Mo}(n, 2n)^{99}\text{Mo}$  reactions in the 7-14 MeV energy range were carried out at Physikalisch-Technische Bundesanstalt, Braunschweig, Germany. The D(d,n) neutron source, characterised by time-of-flight measurements, is well suited for this difficult energy range where significant correction for non-monoenergetic neutrons have to be applied. The radioactivity of the reaction products were determined by means of gamma-ray spectrometry. New data were obtained for the first time in the studied energy range or the knowledge of the excitation functions was improved.

## 1 Introduction

Nuclear data are needed in many fields of science and technology. The safe and economical operation of the modern nuclear facilities requires detailed and reliable design calculations. The accuracy of these calculations is largely determined by the accuracy of the nuclear data input. The development of the new generation fission reactor technologies involve research and innovations in: reactor design, nuclear fuel cycle, safety, waste disposal and transmutation; nuclear safeguards etc. Regarding the design and optimisation of Fusion Nuclear Technology (FNT) facilities accurate data are needed to predict tritium breeding capabilities, power and neutron fluence generation, estimate the long-term shielding efficiency based on the materials activation and radiation damage. Many nuclear applications of growing economic significance have been recently developed, such as: production of radioisotopes for medical and industrial applications, diagnostic and radiotherapy, material research and analysis, detection of concealed explosives and illegal drugs; environmental monitoring, etc. Several national nuclear data centres develop general purpose nuclear data library of evaluated data for utilization in nuclear application design calculations. The development of nuclear data evaluations involves measurements, nuclear model

calculations, nuclear data processing and validations. International organizations, such as International Atomic Energy Agency and OECD Nuclear Energy Agency, provide a framework for co-operation activities on international level. An example of a long-term cooperation in the International Network of Nuclear Reaction Data Centres (NRDC) that has been collaborating on world-wide collection, compilation and dissemination of experimental nuclear reaction data in EXFOR database since 1960s [1].

Molybdenum is considered as alloying element in different advanced nuclear energy system developments due to its excellent material properties at elevated temperatures. Improved quality and completeness of the data base are needed for reliable prediction of the materials behaviour under such conditions. Of particular importance for the integrity of the structural materials is the hydrogen and helium production originating from (n,p) and (n,a) processes. Molybdenum consists of seven stable isotopes. Completeness of the experimental data for Mo isotopes will allow development of nuclear model parameterization in systematic way and validation of the model predictions.

## **2 Activation Cross-Section Measurements**

Activation cross section measurements on Mo isotopes in the 7-15 MeV energy range were carried out at the CV28 compact cyclotron at Physikalisch-Technische Bundesanstalt, Braunschweig. The neutrons were produced by means of the  $D(d,n)^3\text{He}$  reaction, using a gas target of 3 cm length and 1 cm diameter. Gamma-ray spectrometry was applied for the measurements of the activity of the reaction products. Corrections were applied for: contribution of the breakup neutrons, time dependent factors, detector efficiency, gamma-ray self absorption, gamma-ray coincidence summing effects etc.

Neutron beams are produced by various nuclear reactions. The energy and angular distribution of the emitted neutrons are determined by neutron source and irradiation geometry. Very few reactions provide a monoenergetic neutron field and often it covers limited energy range. In the case of  $D(d,n)^3\text{He}$  reaction above 5 MeV incident deuteron energy a breakup of deuteron takes place. The intensity and the energy distribution of the breakup neutrons depend on the incident deuteron energy and steeply increase from the threshold at 5.34 MeV and exceed the production of monoenergetic neutrons for projectile energy above 9 MeV. The neutron spectrum has been characterized by means of time-of-flight measurements using NE213 detector at distance 12 m from the target. The measured neutron spectral distribution was compared with calculated one using Monte Carlo code SINENA, that include data of double-differential cross sections of the  $D(d,np)$  reaction. The detailed study of the  $D(d,np)$  double-differential cross sections at incident deuteron energies from 5.3 to 13.3 MeV and neutron emission angles between 0 and 15 degrees carried out at PTB in the past provided characterization of the neutron production from the deuteron breakup reaction on deuterium [2]. The measured reaction rates of the studied

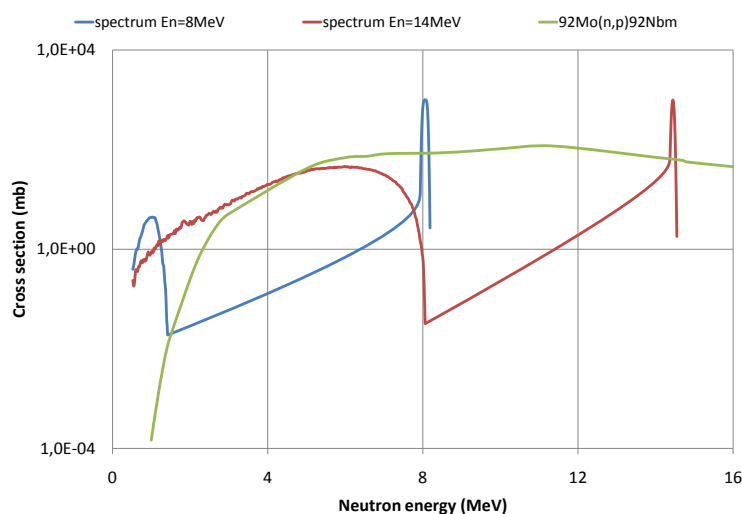


Figure 1.  $^{92}\text{Mo}(n,p)^{92}\text{Nb}^m$  reaction cross-section and histograms of the  $\text{D}(d,n)^3\text{He}$  neutron spectral distribution at two different energies to illustrate the overlap of the breakup neutron energy distribution with the excitation function.

and monitor reactions  $^{238}\text{U}(n,f)$ ,  $^{27}\text{Al}(n,\alpha)^{24}\text{Na}$  were corrected for the contribution of the breakup neutrons by folding the neutron flux distribution with the shape of the excitation function. The output of the SINENA code calculations for the 5.342 and 11.021 MeV incident deuteron energies together with the excitation function of the  $^{92}\text{Mo}(n,p)^{92}\text{Nb}^m$  reaction plotted on Figure 1 illustrate the degree of contribution of the breakup neutrons to the measured reaction rates for this particular reaction.

Efficiency of the HPGe detectors is conventionally determined by measurement of the detector response using monoenergetic gamma-ray standard sources. However, such calibration is valid for the point-like source. A Monte Carlo simulation of the coaxial HPGe detector was performed with the MCNP5 code in order to achieve higher geometry flexibility and better accuracy of the gamma-ray intensity measurements.

The MCNP model of the HPGe detector and the comparison between detector efficiency for the point-like source and calculations for the standard size tungsten sample are presented in Figures 2 and 3 respectively. For samples with high gamma-ray attenuation the assumptions applied for the calculations of the gamma-ray self-absorption correction are not valid and Monte Carlo calculations provide more accurate description of the gamma-ray transport for the particular sample-detector geometry.

An important correction that needs to be applied to the gamma-ray count rates for measurements at close geometry is the coincidence summing correc-

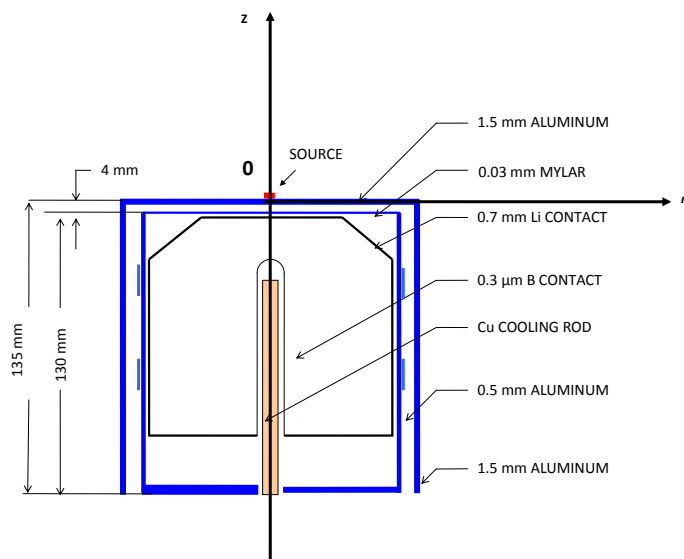


Figure 2. The MCNP model of the HPGe detector.

tion. The gamma-rays emitted in a cascade are sometimes registered as a single event with energy equal to the sum of the energies (full or partial) deposited by the two gammas due to the longer charge-collection response of the detector. A generic formula for coincidence summing correction calculations was published for the first time by Andreev *et al.* [3] and developed by Semkow *et al.* [4] for

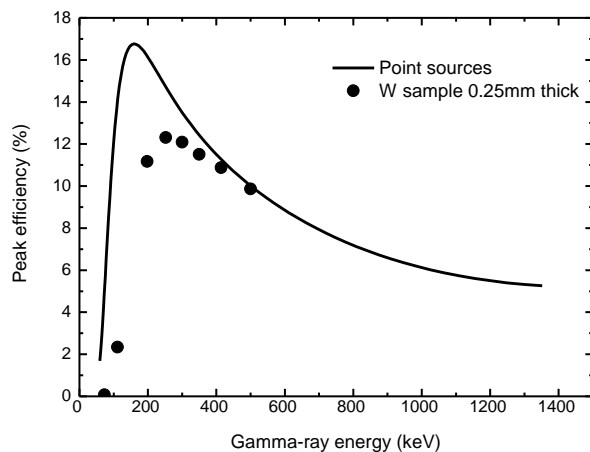


Figure 3. The HPGe detector efficiency for a point-like source and for a standard size tungsten sample.

matrix representation. For a decay scheme with  $n$  levels above the ground state the  $x_{ik}$  is the total branching factor, gamma plus conversion factor ( $\alpha_{ik}$ ), for a transition from level  $i$  to level  $k$ . For all transitions from level  $i$  is valid

$$\sum_{k=0}^{i-1} x_{ik} = 1. \quad (1)$$

The measured gamma-rays peak intensities  $S_{ik}$  in the presence of coincidence summing is obtained from source disintegration rate  $R$  multiplied by terms determined by summing-in and summing-out effects. The term  $A_{ik}$  multiplies the disintegration rate by peak efficiency  $\epsilon_{ik}^p$  to obtain the measured intensities  $S_{ik}$  and at the same time add the contribution from all gamma-rays with total energy equal to  $E_{ik}$ . The terms  $N_i$  and  $M_k$ , being function of  $\epsilon_{ik}^t$ , take into account the summing-out. The direct feeding of level  $i$  and the gamma-transitions above the level  $i$  are accounted for by  $N_i$ , while the coincidences of the measured gamma transition  $E_{ik}$  with the gamma-rays below the level  $k$  are taken into account by the term  $M_k$ .

$$S_{ik} = RN_i A_{ik} M_k, \quad (2)$$

$$N_i = N_{i^*} + \sum_{n=i+1}^m N_n b_{ni}, \quad (3)$$

$$A_{ik} = a_{ik} + \sum_{j=k+1}^{i-1} a_{ij} A_{jk}, \quad (4)$$

$$M_k = \sum_{j=0}^{k-1} b_{kj} M_j, \quad (5)$$

where

$$a_{ik} = \frac{x_{ik} \epsilon_{ik}^p}{[1 + \alpha_{ik}]}, \quad (6)$$

and

$$b_{ik} = x_{ik} \left[ 1 - \frac{\epsilon_{ik}^t}{1 - a_{ik}} \right]. \quad (7)$$

Results of the measurements for some of the studied reactions are shown in Figures 4–7 together with the data from other authors available in EXFOR database [1] and the evaluated data from Evaluated Nuclear Data Files. The decay data used in the analysis are included in Table 1.

Cross-section data for the  $^{95}\text{Mo}(n, p)^{95}\text{Nb}^m$ ,  $^{100}\text{Mo}(n, \alpha)^{97}\text{Zr}$ ,  $^{100}\text{Mo}(n, 2n)^{99}\text{Mo}$  reactions were obtained for the first time in the studied energy range. The new results have improved the knowledge of the  $^{92}\text{Mo}(n, \alpha)^{89}\text{Zr}$  excitation function in the energy range from 8 to 14 MeV.

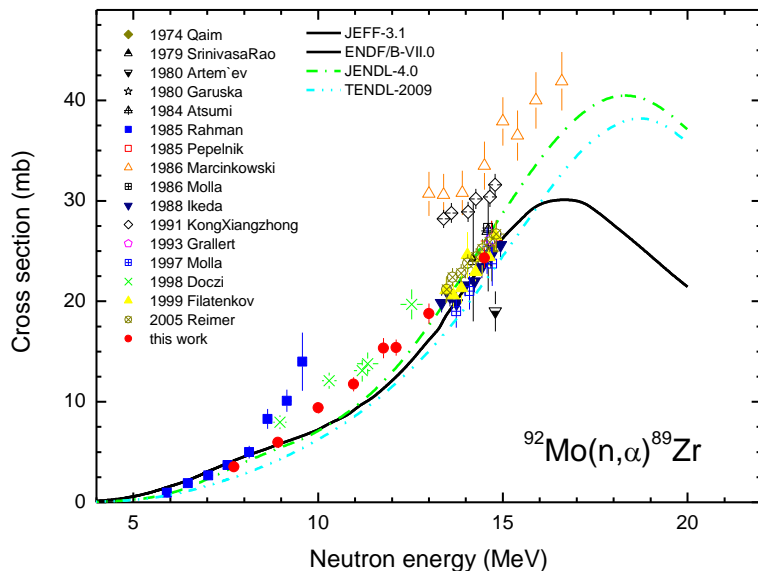


Figure 4. Experimental cross-sections for the  $^{92}\text{Mo}(n, \alpha)^{89}\text{Zr}$  reaction compared with the results from other authors and evaluated data.

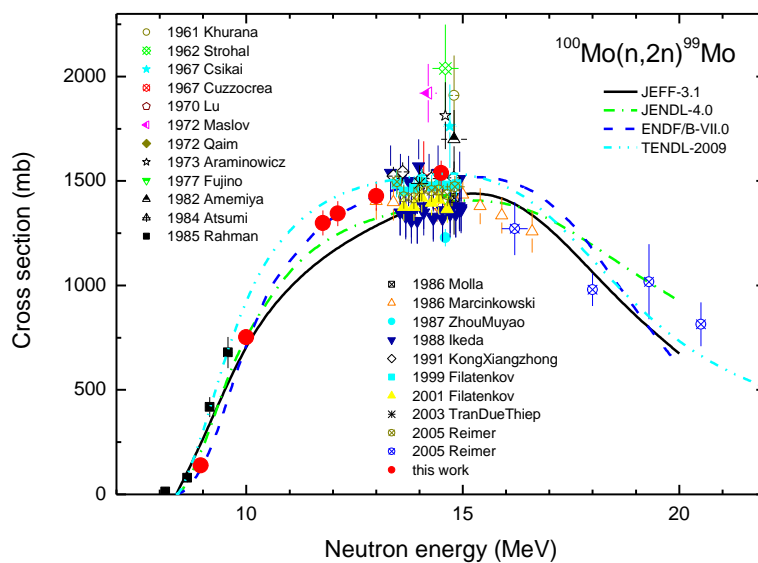


Figure 5. Experimental cross-sections for the  $^{95}\text{Mo}(n, p)^{95}\text{Nb}^m$  reaction compared with the results from other authors and evaluated data.

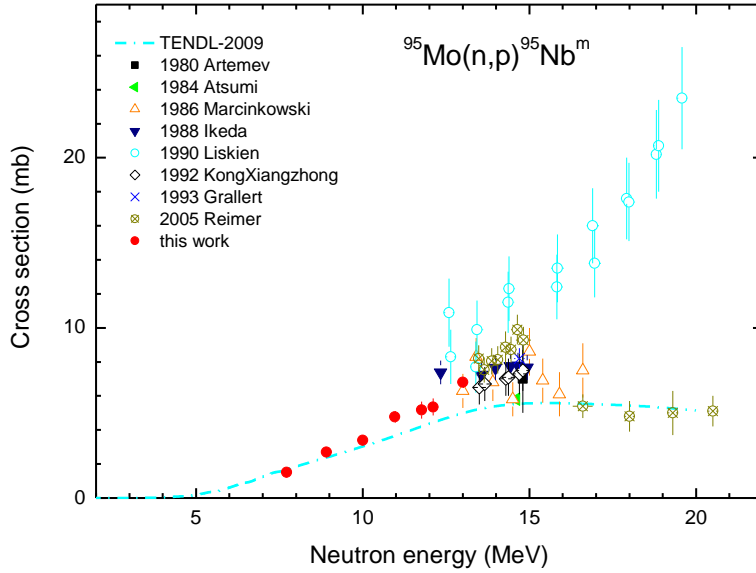


Figure 6. Experimental cross-sections for the  $^{100}\text{Mo}(n, \alpha)^{97}\text{Zr}$  reaction compared with the results from other authors and evaluated data.

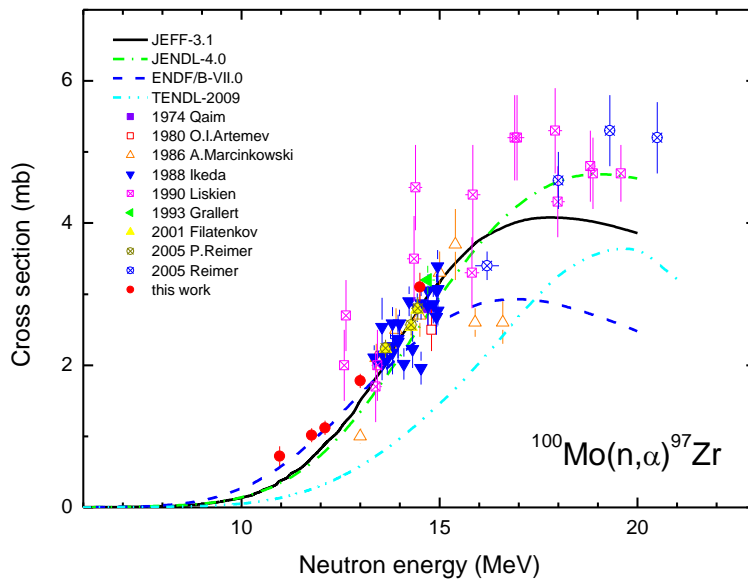


Figure 7. Experimental cross-sections for the  $^{100}\text{Mo}(n, 2n)^{99}\text{Mo}$  reaction compared with the results from other authors and evaluated data.

Table 1. Decay data for the studied reactions

Reaction	Isotopic abundance, %	Half-live	$E_{\gamma}$ , keV	Intensity
$^{92}\text{Mo}(n, \alpha)^{89}\text{Zr}$	14.84	78.41 h	909.15	0.9904
$^{95}\text{Mo}(n, p)^{95}\text{Nb}^m$	15.92	3.63 d	235.69	0.248
$^{100}\text{Mo}(n, \alpha)^{97}\text{Zr}$	9.63	16.744 h	743.36	0.9306
$^{100}\text{Mo}(n, 2n)^{99}\text{Mo}$	9.63	65.94 h	739.5	0.1213

## References

- [1] N. Otuka *et al.*, *Nucl. Data Sheets* **120** (2014) 272-276.
- [2] S. Cabral, G. Boerker, H. Klein W. Mannhart, *Nucl. Sci. Eng.* **106** (1990) 308.
- [3] D.S. Andreev, K.I. Erokhina, V.S. Zvonov and I.Kh. Lemberg, *Bull. Acad. Sci. USSR Phys. Ser.* **37** (1973) 41.
- [4] T.M. Semkow, G. Mehmood, P.P Parekh and M. Virgil, *Nucl. Instrum. Methods Phys. Res.* **A290** (1990) 437-444.